ORIGINAL ARTICLE

Modelling Spontaneous Firing Activity of the Motor Cortex in a Spiking Neural Network with Random and Local Connectivity

Lysea Haggie[1] | Thor Besier[1] | Angus McMorland[1, 2]

[1]Auckland Bioengineering Institute, University of Auckland, Auckland, New Zealand

[2]Department of Exercise Sciences, University of Auckland, Auckland, New Zealand

Correspondence
Lysea Haggie, Level 8 Auckland Bioengineering Institute, The University of Auckland, Auckland, 1010, New Zealanad
Email: lmun373@auckland.ac.nz

Computational models of cortical activity can provide insight into the mechanisms of higher-order processing in the human brain including planning, perception and the control of movement. Activity in the cortex is ongoing even in the absence of sensory input or discernible movements and is thought to be linked to the topology of the underlying cortical circuitry [1]. However, the connectivity and its functional role in the generation of spatio-temporal firing patterns and cortical computations are still unknown.

Movement of the body is a key function of the brain, with the motor cortex the main cortical area implicated in the generation of movement. We built a spiking neural network model of the motor cortex which incorporates a laminar structure and circuitry based on a previous cortical model by Potjans and Diesmann [2]. A local connectivity scheme was implemented to introduce more physiological plausibility to the cortex model, and the effect on the rates, distributions and irregularity of neuronal firing was compared to the original random connectivity method and experimental data. Local connectivity increased the distribution of and overall rate of neuronal firing. It also resulted in the irregularity of firing being more similar to those observed in experimental

measurements, and a reduction in the variability in power spectrum measures.

The larger variability in dynamical behaviour of the local connectivity model suggests that the topological structure of the connections in neuronal population plays a significant role in firing patterns during spontaneous activity. This model took steps towards replicating the macroscopic network of the motor cortex, replicating realistic spatiotemporal firing to shed light on information coding in the cortex. Large scale computational models such as this one can capture how structure and function relate to observable neuronal firing behaviour, and investigates the underlying computational mechanisms of the brain.

1 | INTRODUCTION

The motor cortex is critical for producing movement. However, neurons in the motor cortex show patterns of ongoing activity even during resting state periods with no discernible movement [3]. Baseline spontaneous activity, which is observed in awake and conscious experimental subjects, is differentiable from task-induced states in recordings of neuron spiking behaviour [4, 5, 6, 7]. Spontaneous activity of the brain at rest has spatially structured patterns of activity and is considered to play an important role in neural encoding for brain processes [1, 8]. Previously, activity in the cortex was thought to be driven by external sensory input, but it recently has been suggested that spontaneous activity arises from the dynamics of the neuronal circuitry and inputs modulate and modify the dynamics of the network rather than drive it [9, 10]. Thus, there is an interest in understanding the ongoing behaviour of neural activity, how it reflects the cortical circuitry and shapes the variable functions of the cortex [11, 9, 12].

Spontaneous activity in the motor cortex, similar to other cortical areas, is characterised by irregular firing of individual neurons, with low average firing rates (< 10 Hz) but a wide frequency range (0 - 100 Hz) [4, 13, 14, 15, 16]. Firing rates in cortical networks measured *in vivo* are reported to have highly positively skewed, long-tail distributions [17]. Neuron populations in the cortex also display oscillatory firing activity covering a broad frequency spectrum ranging from less than one hertz to hundreds of hertz [18, 13]. In the motor cortex, beta oscillations (13–30 Hz) are consistently observed in electroencephalography (EEG) measurements during resting states or prior to movement, and disappear during movement [19, 20].

The origin of the variability in the firing of cortical neurons is unknown and could be due to morphology of dendrites resulting in non-linear integration of inputs, or the properties of the network and synaptic coupling [21, 22, 23, 24]. The variability in neuronal activity is also believed to play a significant role in information encoding in the cortex [25, 26, 27]. Recently, the generation of neocortical activity has been addressed through computational models of somatosensory cortical circuits based on anatomical and physiological data, which generate realistic spontaneous dynamics [28, 2]. However, specific model structure or features have not been clearly linked to cortical firing patterns.

The cortex is thought to have a consistent laminar organisation and patterns of connectivity across different regions [29, 30, 26]. A canonical circuit which generally defines recurrent connections in each layer, layer 4 and 6 as input layers,

and layers 2/3 and 5 as output layers, was based originally on Hubel and Wiesel [31]'s work on the cat visual cortex and a similar pattern observed in other cortical areas in primate studies including the auditory cortex, somatosensory cortex and motor cortex [29, 32, 33, 30]. Binzegger et al. [34] quantified connectivity of the cortical circuit through *in vivo* intracellular recordings and morphometry of cell types and laminar distribution. This and other photostimulation and optogenetic studies of the mouse motor cortex have shown a dominant connection of layer 2/3 neurons to layer 5 neurons [35, 36, 37].

Experiments involving *in vivo* extracellular injections of neuronal tracers in the cortex observe 'patchy' projections, in which synapses are highly localised [33] (also see Voges et al. [38] for review). Recent photostimulation experiments and digital image reconstruction suggest a distance-based connectivity model with strong connectivity within 0.2 mm of the soma and connectivity decreasing as a function of distance [39, 40]. Diffusion tensor imaging also shows small-world, patchy connections in the cortex and greater local connectivity than "random" connections [41]. Localised connections are also thought to be optimal in regards to minimising wiring but maximising connectivity between nodes in a network. Local connections with some long range connections may be an efficient method of information transfer in the brain [38]. Structural variations in network topology influence the spatio-temporal activity of the cortex, with changes in connectivity patterns resulting in different dynamics [42].

Large-scale neural network models can be used to explore how network structure influences the generation of cortical activity. Voges et al. [38] modelled the horizontal connectivity in the neocortex and showed complex activity patterns arise in structured, spatially clustered synapses. There recently has also been the development of larger-scale cortical models which contain tens of thousands of spiking neuron models [43, 2]. However, previous models of the motor cortex have been limited in replicating physiological detail and mainly been focused on generating movement dynamics or responses to stimulation [44, 45, 43, 46]. The role of network connectivity in generating spontaneous cortical activity in physiologically-based spiking neural network models has not been explored.

Computational models can aid in the understanding of the electrophysiological mechanisms which underlie the generation of spontaneous activity. In this study, a large-scale spiking neural network containing over 38,000 neurons and 150 million synapses, based on previous modelling work by Potjans and Diesmann [2], was implemented in the Python-based neural network simulator, Brian2 [47]. The model was developed to replicate the spontaneous firing behaviour of the motor cortex and explore the effect of local connectivity on the network behaviour. The aim of this work was to provide insights into resting state motor cortex dynamics using a spiking neural network model and investigate connectivity as a potential source of variability and efficient information transmission in spontaneous firing behaviour.

2 | METHODS

This model was based on previous work by Potjans and Diesmann [2] and implemented in Brian2 with reference to source code from Shimoura et al. [48]. The original cortical circuit model was adapted to represent a 1 mm^2 surface area of the motor cortex. The model follows a laminar structure, grouping the neurons into four layers, 2/3, 4, 5, and 6. Each layer was further divided into excitatory and inhibitory cell groups. Layer 1 was ignored due to its low density of neuronal cell bodies [49]. Connection weights in the circuit are shown in figure 1 below.

Individual neuron dynamics were governed by leaky-integrate-and-fire equations simulated using the linear state updater with a time step of 0.1 ms. Equation 1 describes the membrane potential (V) of each neuron, where τ_m is the time constant, C_m is the membrane capacitance, V_r is the reset value for the membrane potential following a spike and I_{syn} is the total input current described by equation 2. Action potentials were fired whenever Vt became more positive than the threshold (θ). On the firing of a presynaptic neuron, the synaptic current of the postsynaptic neuron

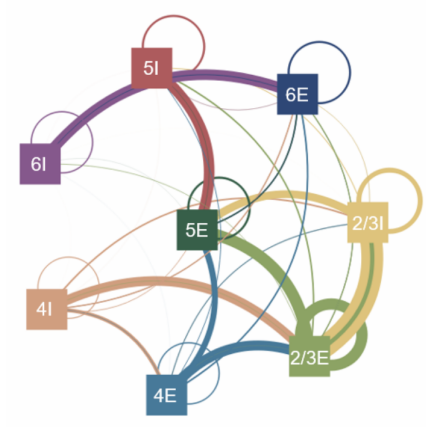

FIGURE 1 Circuit diagram of the motor cortex model showing connections between the populations of excitatory (E) and inhibitory (I) neuron groups. Groups are organised according to their layer. The colour of the lines indicates the source group. Thickness represents the relative number of connections and weighting of synapses.

(I_{syn}^{post}) was changed by the value determined by the conductance (g) multiplied by the weight (w) after a delay (d) which accounts for the finite time interval of an action potential propagation in a presynaptic neuron (equation 3). The delay between the spiking activity of a presynaptic neuron and postsynaptic neuron was drawn from a normal distribution with a mean of 1.5 ms for excitatory neurons and 0.8 ms for inhibitory neurons; the standard deviation of delay times was half of the mean value. A shorter inhibitory delay was used in the model as inhibitory neurons generally make more local connections over smaller distances [50, 51, 52, 53, 54]. In unmyelinated axons, each millimetre could introduce a conduction delay of at least 2 ms [55]. Cortical neurons exhibit a range of myelination, though inhibitory interneurons also show more myelination, thus also potentially increasing conduction speed [56]. Our model only incorporated 1 mm of cortical area and so delays were defined as less than 2 ms with shorter delays for inhibitory neurons, and were also independent of layer as in Potjans and Diesmann [2]. Following a spike being fired, the membrane voltage was reset to -65 mV. The refractory period of the neuron was 2 ms meaning another spike could not be fired within that period of time following a previous spike. As in the original Potjans and Diesmann [2] model, the conductance value in the layer 4E to layer 2/3E connection was doubled compared to the other excitatory connections. Parameter descriptions and values are given in table 1.

$$\frac{dV\left(t\right)}{dt} = \frac{-V\left(t\right) - V_r}{\tau_m} + \frac{I_{syn}\left(t\right)}{C_m} \tag{1}$$

$$\frac{dI_{syn}}{dt} = -\frac{I_{syn}}{\tau_{syn}} \tag{2}$$

TABLE 1 Parameters for neuron model. Taken from Potjans and Diesmann [2].

Symbol	Name	Value
C_m	Membrane Capacitance	250 pF
θ	Threshold	-50 mV
τ_{ref}	Refractory Time	2 ms
τ_m	Membrane Time Constant	10 ms
τ_{syn}	Synaptic Time Constant	0.5 ms
V_r	Reset Value	-65 mV
g_e	Excitatory Conductance	1
g_i	Inhibitory Conductance	-4
w	Synaptic Weight	87.8 pA
d_e	Mean Excitatory Delay	1.5 ms
d_i	Mean Inhibitory Delay	0.8 ms

TABLE 2 Neuron groups in the motor cortex model, the proportions of neurons in each group (kept constant in sensitivity analysis), and absolute number of neurons in each neuron group in the final model.

Group	2/3E	2/3I	4E	4I	5E	5I	6E	6I
Proportion	0.268	0.076	0.063	0.014	0.284	0.071	0.187	0.038
Absolute	10332	2916	2412	540	10944	2736	7200	1476

E, excitatory; I, inhibitory. Number indicates cortical layer.

$$I_{syn}^{post}\left(t+d\right) = I_{syn}^{post}\left(t+d\right) + g \cdot w \quad \text{when presynaptic neuron } \mathrm{V(t)} \geq \theta \tag{3}$$

Neurons were distributed over eight populations, according to the numbers in table 2. Neuron numbers were adjusted from the original Potjans and Diesmann [2] model, switching the proportion of layer 4 and 5 cells based on the motor cortex having a dominant layer 5 connectivity and sparser cell distributions than other layers of the cortex (ie. the somatosensory and visual cortices on which the original model was based) [57]. Previously, the motor cortex has thought to lack a distinct layer 4 but recent studies support a functional, albeit small, layer 4 in the motor cortex with similar connections to layer 4 in the somatosensory cortex, notably as an input pathway from the thalamus [58, 59]. The superficial layers of 2/3 and 4 contain approximately 40% of the neurons, layer 5 has 35% of the neurons and layer 6 has 25% of the neurons, which is similar to reported physiological experimental data [60]. The E/I ratio in this model is on average 24%. With inhibitory neurons making up 28.2% 24.8%, 22.4%, 20.5% for layers 2/3, 4, 5 and 6, respectively. The proportion of GABA cells in motor area has been reported as 24.2% with slightly lower percentage of GABA in deeper layers [61]. A sensitivity analysis was carried out to investigate the effect of the total number of neurons in the network, to select a minimal number of neurons at which the rate and irregularity of firing activity converges.

TABLE 3 Connectivity probability values (C_a) used in equation (4) to determine the number of synapses (K) between each group.

	Source Group							
Target Group	**2/3E**	**2/3I**	**4E**	**4I**	**5E**	**5I**	**6E**	**6I**
2/3E	0.192	0.3095	0.3356	0.5802	0.0143	0	0.0159	0
2/3I	0.252	0.2553	0.2558	0.4183	0.034	0	0.008	0
4E	0.016	0.012	0.3725	0.7704	0.0031	0	0.0879	0
4I	0.1334	0.006	0.5266	0.8295	0.0013	0	0.2007	0
5E	0.1902	0.1202	0.3785	0.0592	0.0377	0.1662	0.0396	0
5I	0.1071	0.0533	0.2129	0.0201	0.027	0.1374	0.0179	0
6E	0.0318	0.014	0.1754	0.1597	0.0257	0.0078	0.0784	0.399
6I	0.0708	0.002	0.0269	0.0101	0.0125	0.0031	0.1276	0.267

E, excitatory; I, inhibitory. Number indicates cortical layer.

Potjans and Diesmann [2] original connectivity map integrated the findings of multiple anatomical and electrophysiological studies to estimate the probabilities of connection and number of synapses formed between each neuron group. Combining these data from different species and areas, including rat visual and somatosensory areas and cat visual striate cortex, builds on the theoretical framework suggesting an equivalency across cortical areas. Comparative studies of primary motor cortex also show functional preservation across mammals [62]. The connectivity profile was based on a modified version of Peter's rule which proposes that the number of synapses is dependent on the number of neurons collocated in the presynaptic and postsynaptic layers and a probability value of connection between layers, derived from experimental data [63, 64, 34, 65].

Based on Peter's rule and probabilities derived from anatomical and physiological studies, the number of connections (K) was calculated for neuron groups using equation 4 (Equation 3 in Shimoura et al. [48]) where C_a is the connection probability defined in table 3, and N_{pre} and N_{post} are the sizes of the presynaptic and postsynaptic populations, respectively. The C_a values in the connectivity matrix (Table 3) describing the probabilities of connections between groups were adapted from the original Potjans and Diesmann [2] study in this motor cortex model based on changes to the number of neurons in each layer, while maintaining the average relative number of connections in each neuron target group as the original model. The resulting connectivity was similar to experimental investigations of layer specific wiring in the motor cortex [35], notably the dominant layer 2/3 to layer 5 connection pathway (Figure 2).

$$K = \frac{log\left(1 - C_a\right)}{log\left(1 - \frac{1}{\left(N_{pre}N_{post}\right)}\right)} \tag{4}$$

The original Potjans and Diesmann [2] cortical model implemented a random connectivity scheme. This was reimplemented and adapted here to model the motor cortex, as described above, and a new local connectivity scheme was developed. In the random and local connectivity schemes, the total number of synapses in both models was kept constant for fair comparison. Neurons were given spatial parameters (X, Y, and Z coordinates) to be distributed over a

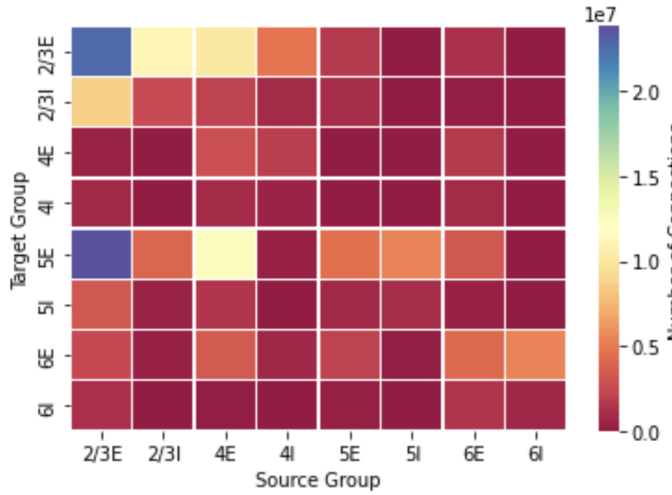

FIGURE 2 Connectivity matrix of neuron populations in the model

TABLE 4 Connection radius for various connection types

Connection Type	Radius (μm)
Horizontal Intralaminar Excitatory Connections (Layer 2/3, 4 & 5)	300
Horizontal Intralaminar Excitatory Connections (Layer 6)	225
Vertical Interlaminar Excitatory Connections	50
Inhibitory Connections	175

1 mm^2 surface and a depth range based on the group's layer. The likelihood of a neuron connecting with another neuron was determined by a Gaussian distribution over distance, where x and y are a neuron's spatial location and the $radius$ parameter defines the extent of the spread (Equation 5). This connectivity is compatible with the synapse definition of the original random model described earlier but the added spatial description of neurons allowed constraining the synapses to a localised connectivity. The spatial connectivity description was also adapted from previous cortical modelling work [66, 67, 43]. Intralaminar connectivity had a greater radius of connectivity than interlaminar connectivity and inhibitory connections had a lower connectivity radius than excitatory connections as supported by physiological data [39, 68, 54, 69]. The radius value for different connection types is given in table 4. Multiple connections could be established between two neurons in both the random and local connectivity schemes and self connections in the local connectivity model were not allowed. Figure 3 shows the postsynaptic connections of a single neuron (red) on the random connectivity model and the connectivity of a single neuron in the distance based connectivity model.

$$Probability = exp\left(-\frac{{x_{pre} - x_{post}}^2 + {y_{pre} - y_{post}}^2}{2 * radius^2}\right) \tag{5}$$

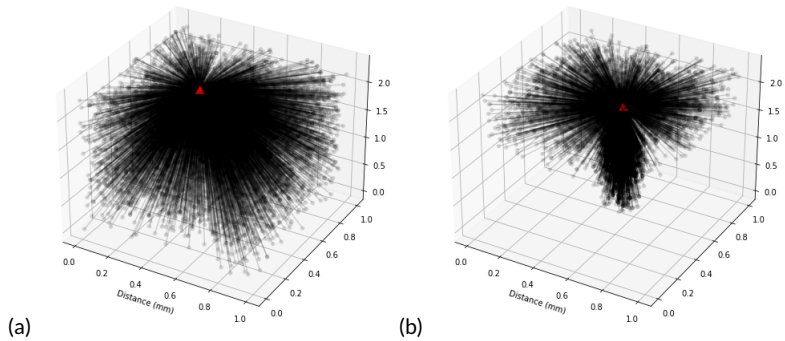

FIGURE 3 Connectivity of a single excitatory neuron on layer 2/3 (a) random connectivity (b) local connectivity. Model represents $1mm^2$ of cortical surface. Units along all axes are in mm.

External input was applied to each neuron group as Poisson spike trains at a frequency of 8 Hz. The number of these inputs for each neuron was constant at 2000 inputs for excitatory neuron groups and 1850 inputs for inhibitory neuron groups. This followed the layer-independent input protocol from the original Potjans and Diesmann [2] model. A sensitivity analysis on the effect of the input on the resulting firing rates was also performed by manipulating the number of inputs and frequency.

To characterise the activity of the network, spike trains and firing rates of neurons and neuron groups were monitored. A spike was defined by the neuron reaching the threshold value of -50 mV. Firing rates were calculated by counting the total number of spikes in each time step of the simulation (0.1 ms). Simulations were run for 500 ms and the first 50 ms was ignored to allow the model to reach steady state. The interspike intervals (ISIs) for each neuron were calculated as the time between spikes. Irregularity was characterised by the coefficient of variation (CV) of the ISI distribution. CVs were calculated as the ratio of the standard deviation to the mean ISIs (Equation 6) for each individual neuron in the population, as defined previously [48, 2]. Firing rates and CVs reported are the mean across neurons in the neuron group, and over time. Notably, firing rates and CVs closely matched values reported by the original model when the settling period was included, consistent with the analyses conducted by Shimoura et al. [48], but due to the inconsistency in the spiking behaviour in the first 50 ms, this settling period was excluded for the analyses carried out in this study.

$$CV = \frac{\sigma_{ISI}}{\mu_{ISI}} \tag{6}$$

3 | RESULTS

The motor cortex receives connections from multiple brain regions such as the thalamus, premotor cortex and somatosensory cortex; this complexity makes selection of an appropriate surrogate input challenging. The effect of the input number and frequency to the model was explored while keeping the ratio of excitatory and inhibitory input and relative input between the different neuron groups constant (ie. 2000 for excitatory neurons, 1850 for inhibitory neurons). A single input frequency was used across the model though physiologically there may be variation in the number of inputs and range of input frequencies. Networks with local connectivity show greater sensitivity to the

frequency and number of inputs, with a greater range of resultant average firing rates. Figure 4 shows a heat map of the effect of input number and frequency on the average firing rates of neurons in the model, note the change in scale in each colour map.

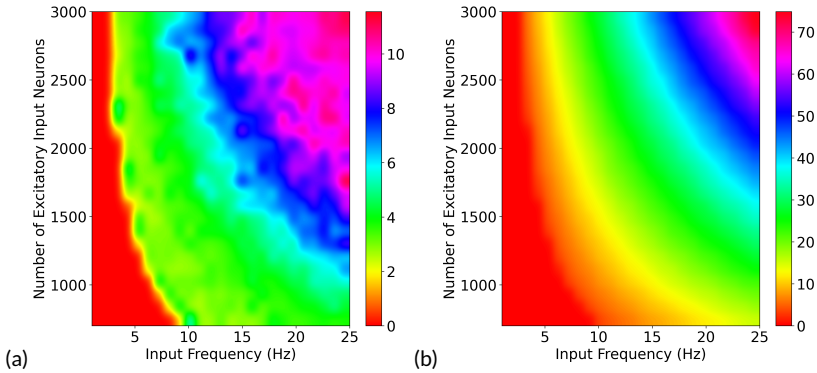

FIGURE 4 Average firing rates in model with changes to input number and frequency for (a) random connectivity and (b) local connectivity. Inhibitory neuron inputs were kept proportional at 92.5% of excitatory inputs. Scales represent average firing rate across all neurons. Note the different range in scales of the colour maps.

An analysis of the effect of the number of neurons in the model showed that consistent frequencies and CVs were produced by a random network containing 35,000 or more neurons. Neuron counts by isotropic fractionator and flow fractionator methods of the motor cortex in old and new world primate species lie in the estimated range of 50,000–90,000 neurons per mm^2 [57, 70]. Figure 5 shows the firing rates and CVs in the network over a range of 0–80,000 neurons for both random and local connectivity, with standard deviation measures over ten simulations. The firing rates and CVs were more stable in the local connectivity model at lower number of neurons. In both models, layer 6E neuron CVs were not able to be calculated or were highly variable, probably due to very low firing rates in the neuron group, and were thus excluded from the figures.

The firing rates of the model were within an appropriate range of baseline physiological recordings of a number of studies, with lower firing rates in layer 2/3 and layer 6 of the model than layer 5 [71]. Beloozerova et al. [72] presented microelectrode measurements of the motor cortex in awake rabbits, with mean discharge rates of 0.6 Hz in corticocortical neurons, prevalent in layer 2/3, 5.7 Hz in layer 5 neurons and 0.4 Hz in layer 6 neurons. Schiemann et al. [73] published similar values from whole cell patch clamp recordings in mice. Dabrowska et al. [4] recorded firing rates in two awake monkeys and firing rates in a resting state were 6.3 Hz and 7.81 Hz and CV measures of 0.83 and 0.79 which lies closer to the irregularity of a random poisson distribution (CV = 1). These were recorded using a 100 electrode Utah Array in the hand motor area of macaque monkeys, at a depth of 1.5 mm, which would correspond to deep layer 3 or superficial layer 5 [74]. Lacey et al. [15] reported a similar mean value of 7.1 Hz firing in layer 5 motor cortex cells at rest, from micro-electrode recordings in rats. CVs of spiking activity in cortical neurons have been consistently reported in previous literature as being close to 1 [75, 76].

Based on these experimentally reported values, the firing rates of the neural network model with random connectivity were closer to the physiological range, though with slightly higher firing in layer 2/3 and lower in 6. The local connectivity model showed an increase in mean firing rates over all the neuron populations and a wider range in mean CV. The mean CV values in the local connectivity model more closely matched experimental recordings in the middle-deep layers, notably in 5E which is the dominant neuron group. Firing frequencies were also observed to

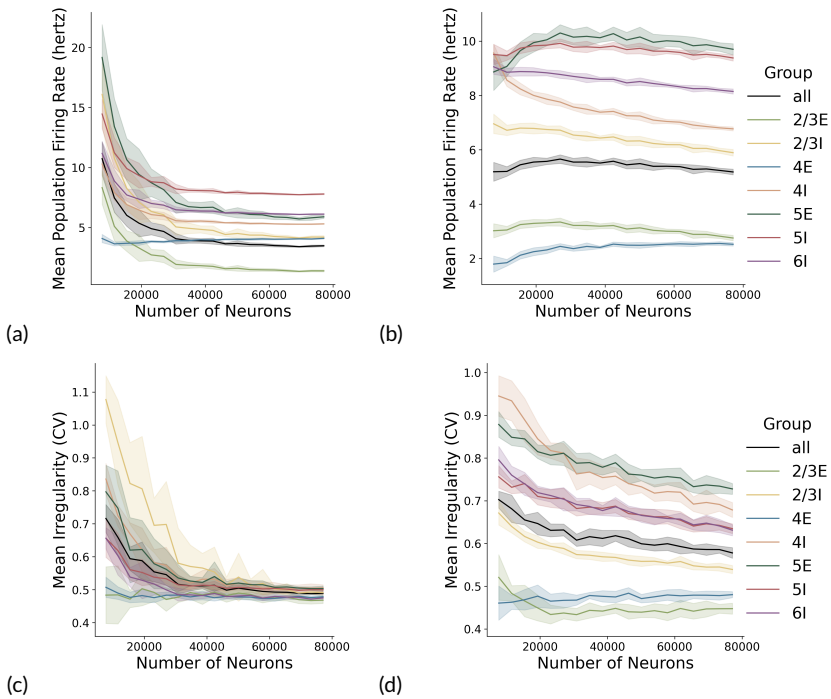

FIGURE 5 Numerical sensitivity analysis for firing rates of neuron groups in (a) random connectivity and (b) local connectivity, and the coefficient of variation in neuron groups with (c) random connectivity model of the motor cortex and (d) local connectivity. The proportions of each neuron group and relative number of synapses were kept the same.

TABLE 5 Mean firing rates and coefficient of variability, with standard deviations, of neuron group activity in random and local connectivity schemes.

	Random Connectivity				Local Connectivity			
Neuron Group	Mean FR (Hz)	STD FR	Mean CV	STD CV	Mean FR (Hz)	STD FR	Mean CV	STD CV
2/3E	1.86	8.44	0.51	0.27	3.24	6.98	0.42	0.21
2/3I	4.81	11.78	0.56	0.26	6.57	8.81	0.57	0.25
4E	3.99	7.44	0.48	0.24	2.55	5.25	0.48	0.23
4I	5.51	12.97	0.51	0.24	7.42	14.71	0.75	0.28
5E	6.90	15.16	0.58	0.24	10.51	10.87	0.79	0.27
5I	8.13	9.22	0.51	0.22	9.90	10.49	0.67	0.26
6E	0.008	0.034	-	-	0.125	0.59	0.55	0.27
6I	6.42	9.10	0.51	0.22	8.66	10.96	0.67	0.25

FR, Firing Rates; STD, Standard Deviation; CV, Coefficient of Variability; E, Excitatory; I, Inhibitory

be higher in inhibitory neuron groups. Table 5 reports the mean values and standard distributions of firing rates and irregularity (CV) in the random connectivity model and local connectivity model.

The activity of neurons in the model showed a different pattern of activity in the local connectivity model compared to the random connectivity. Figure 6 shows a raster plot of 10% of the neurons in the model and a plot of the frequencies across the neuron groups. Firing rates of the neuron groups generally remained $<$ 100 Hz but the random connectivity model showed a greater tendency for sudden high frequency firing activity across the network. This synchrony of firing activity could be neuronal avalanches, bursts of firing, which are a noted feature of brain dynamics and indicator of scale-free critical dynamics in complex systems [77].

The range of firing rates in recorded neurons also varies with long-tailed distributions of firing rates [17]. The range of firing is reported to be 0–40 Hz in measurements of awake mice and cats [78, 79], while recordings in monkeys ranged from 0–100 Hz [4]. The firing rates of the model also showed long tailed distributions (Figure 7), with longer tailed distributions, closer to physiological data, in the local connectivity model.

A power spectrum analysis shows a peak between 10–30 Hz which lies within the beta oscillation range (13–30 Hz). Experimentally, beta waves are observed by EEG, magnetoencephalography (MEG) or electrocorticography (ECoG), though the origin and role of this rhythm is still unclear [80, 24, 81, 82]. This model suggests that oscillatory rhythms could be emergent properties of the cortical network since the input to this model is non-oscillatory. The standard deviation, taken over ten simulations, was slightly reduced in the local connectivity model suggesting a potential regularisation of the power spectrum and beta peak (Figure 8).

4 | DISCUSSION

This study builds on previous cortical modelling work, and investigates the effects of a physiologically-realistic, spatially defined local connectivity scheme on neuron activity, while focusing on replicating the spontaneous firing in the motor

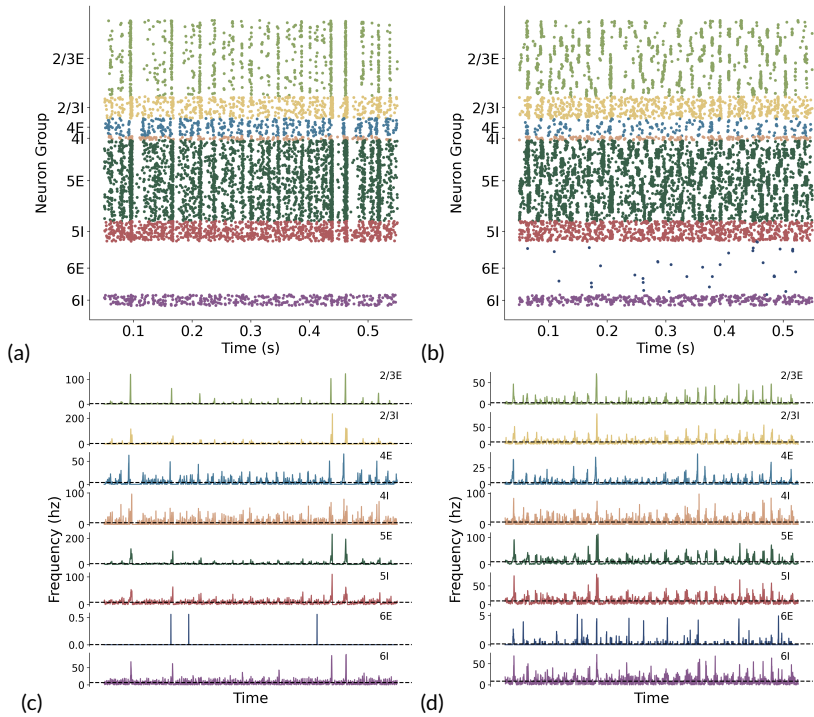

FIGURE 6 Raster plots of the model spiking behaviour with (a) random connectivity and (b) local connectivity. Population rates of model with (c) random connectivity and (d) local connectivity.

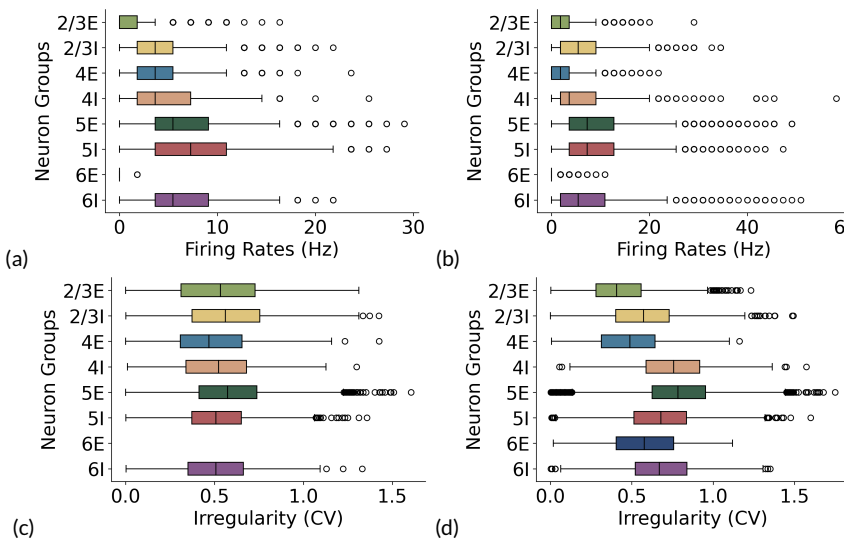

FIGURE 7 Firing rates box and whiskers for (a) random connectivity and (b) local connectivity. Irregularity (CV) box and whiskers plot for (c) random connectivity and (d) local connectivity.

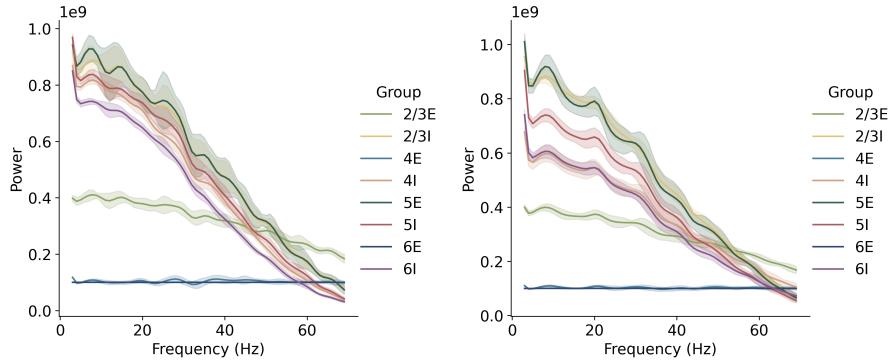

FIGURE 8 Power spectrum of random (left) and local (right) connectivity with observed beta 'peaks' between $10 - 30$Hz.

cortex. We replicated spontaneous firing behaviour in regards to neuron firing rates, irregularity, and power spectrum peaks, as recorded by previous experimental data. Local and random connectivity was compared in the model to provide insight to the topological network properties that influence population-based firing behaviour. Local connectivity showed qualitatively different temporal patterns of firing and more realistic irregularity (CV). It also resulted in a wider tailed distribution of firing and a narrower standard deviation in the power spectrum.

Spontaneous activity in the cortex has been characterised by low firing rates and asynchronous activity. The model with random connectivity replicated previously measured values with lower firing rates in layers 2/3 and 6 and higher firing rates in layer 5. The increase in firing rates in the local connectivity model may be due to more coordinated inputs within a local cluster resulting in a greater likelihood to reach threshold. This could be broadly explained by the theory of neurons as coincidence detectors, which states that information is encoded and propagated by the timing of action potentials [21, 83, 84, 85]. Though local connectivity increased the firing rates of the network, similar proportions of firing rate values between layers were maintained, which suggests additional tuning of input or overall connectivity density might resolve the differences in absolute firing rate and be able to reduce firing to match experimental results.

The local connectivity model replicated experimentally derived CV values in the deeper layers of 5 and 6, with similar CV values to the random connectivity model in the superficial layers 2/3 and 4. As such, the topological structure played a key role in the variability of firing activity. The local connectivity model also exhibited a lower standard deviation in the power spectrum, compared to the random connectivity model. The narrower range in the power spectrum suggests a more reliable occurrence of beta wave frequencies that are consistently observed in EEG recordings. The more realistic, local connectivity model could therefore be a topological pattern in the cortex which contributes to the occurrence of the beta wave.

Compared to the random connectivity model, the local connectivity scheme showed more sensitivity and instability in response to input activity. Within the range of changes in the input, the local connectivity model covered a larger range of frequencies in the firing behaviour of the network. The greater sensitivity to input could be a key factor in the highly variable activity in the cortex which might be necessary for phase transitions or changes in state, a notion described by criticality [86, 77, 87, 88]. This critical state is hypothesised to be functionally beneficial for efficient information transmission in the cortex [89]. In the motor cortex, being in the critical state may play a role in the generation of a wide range of voluntary muscle movements.

The E/I ratio is critical in determining the model dynamics and emergent behaviour [90, 91]. The balance of E/I

activity is linked to scale-free dynamics and operating near a critical point of activity, which does not extinguish or explode into seizure [92, 89]. The overall level of excitation and inhibition, as well as the detailed dynamics of excitatory and inhibitory synaptic conductance, has a large effect on circuit activity. Our model contained 24% excitatory neurons, with post-synaptic conductance of inhibitory connections modelled with a conductivity 4 times stronger than excitatory connections, resulting in a stable E/I balance. However, this E/I ratio could be an area of further exploration as recently a study by Bakken et al. [62] looked at rat, marmoset and human cell types and found a proportion of GABAergic neurons as 16% in mouse primary motor cortex, 23% in marmosets and 33% in human primary motor cortex.

The random connectivity model has been used in previous studies of cortical dynamics [93, 94]. Random networks are less clustered in their connections, have longer range connections, and are considered to be inefficient with regards to information transfer [95]. Mehring et al. [96] implemented a locally connected random network (LCRN), with distance-based connectivity in a large scale neural network model containing 100,000 neurons. Kumar et al. [92] also used a LCRN to investigate the propagation of synchronous and asynchronous activity. Typically, these models have two populations, excitatory and inhibitory neuron groups with recurrent intra- and inter-group connectivity. Previous investigations of connectivity have been limited to 2D networks which have not aimed to replicate physiological behaviour [97, 98]. However, to further investigate the spatio-temporal activity of the cortex, particularly with longer range connections, across a cortical network a larger spatial surface area is still needed and this will require increased computing power.

Whether the connection of neurons in the cortex are specific or random has not yet been fully resolved, though recent studies have suggested that neuron morphology and patterns of recorded activity support a notion of specific connections [99, 100]. Axons do not simply connect to neurons based on spatially overlapped locations but selectively target specific neuron types or groups, for example in layer-specific connectivity patterns [99, 101]. There also appears to be both local and long-range connections in the cortex which is suggested to be efficient in regards to wiring cost and information transfer [38, 98]. A combination of short and long-range connections were included within the local connectivity model with horizontal, intralaminar connections spanning the surface area of the model, while vertical, interlaminar connections were narrower in radius.

Over 70 years ago, Mountcastle [102] made experimental recordings of neurons in the cat somatosensory cortex and proposed an organisational unit of a 'vertical group of cells extending through all cortical layers' known as a *cortical column*. Columns are groups of neurons, in the range of 0.5 mm in diameter, tuned to a specific stimulation or attribute in the range of 0.5 mm in diameter, with the arrangement of columns patterned like a 'mosaic' [103]. However, the function of this columnar organisation remains unclear and there is still no agreed upon function or definition [104, 105, 103]. In the motor cortex, recordings of neurons show directional tuning during upper limb movements with activity [106]. Multi-unit recordings also support functional clusters which exhibit directional tuning, with widths of the tuning field reported in the range of 50-250 μm in diameter [107, 108, 109]. Individual neurons can make connections outside of columns, with horizontal connections spanning up to 1.5 mm [68]. Although this model only represented 1 mm^2 of cortical surface area, future development could explore an area representation with and without an added constraint to model cortical columns. The topographic structure of the motor cortex and its relation to muscle movement parameters is still undefined and with this model, we can begin to explore these intricate connections in the motor cortex.

The effect of neuron types on cortical dynamics might also be an interesting area for future investigation using this model. Spontaneous activity may physiologically reflect a wider range of neuron types or synaptic dynamics, such as bursting or faster and slower transients, than the simplified excitatory and inhibitory neurons captured in this model [11, 110, 111, 112, 13]. The diversity of inhibitory interneurons also plays a significant role in the modulation of cortical dynamics, though there still currently lacks a clear consensus on the classification of neurons [113, 50]. Though our model incorporated a simplified model of neuron dynamics and input, we showed that more realistic patterns of spontaneous activity can be replicated in a cortical circuit with local connectivity. Incorporation of different cell types

would certainly have dynamical consequences at the network level.

Our approach increases the biological plausibility of previous cortical modelling work and contrasts with previous models of the motor cortex which have used continuous-value recurrent neural networks [114, 115]. We recognise that we have not considered other properties such as neuron types, dendritic processing and synaptic plasticity that are likely to play a role in firing dynamics. Biological learning paradigms such as reinforcement learning with spike-timing dependent plasticity (STDP) have previously been incorporated in spiking neuronal models of motor control, though not specifically replicating motor cortex activity [116]. Concurrently, experimental data will also be vital for continued model development and validation, a synergy of computational and experimental techniques will be required to elucidate the complex connectivity of cortical circuits and how it contributes to the generation of dynamic activity.

This work is the beginning of a larger scale exploration of neural control in the motor system with scope to extend the model. The proposed model could be incorporated into feedforward and feedback circuits in the neuromusculoskeletal system involving the spinal cord and alpha-motoneuron pools. Motor-unit and muscle recruitment might be task-specific [117], however, the role of the motor cortex in executing movement commands has not yet fully been elucidated. Our model could be used to explore the generation of muscle activity [118]. The model could also fit into a thalamocortical circuit framework to explore mechanisms of movement generation [119]. Dynamical motifs in the activity could be further explored through dynamical systems frameworks, incorporating dimensionality reduction techniques to look at patterns of 'trajectories' in neural population activity which may be task-specific [6, 120].

In summary, the implementation of a local connectivity scheme in a spiking neural network model has shown that the topology of the network plays a critical role in the resulting cortical dynamics. Our results support theories of structured cortical circuitry and local, patchy connectivity in the generation of spontaneous activity patterns in the motor cortex. Random networks appear to be more regular or synchronous in their behaviour, while the local connectivity model showed more realistic irregularity, particularly in the large pyramidal, output neurons of layer 5. Our model builds on previous work incorporating local connectivity in a more complex laminar structure and cortical circuit, and reproduces firing patterns comparable to those measured *in vivo* in the motor cortex. The output from our model indicates the importance of including physiologically-based local network topology, which resulted in an increased range and irregularity in firing as well as a slight regularisation in the power spectrum, compared to a random network.

5 | CONCLUSION

In developing this model, we have aimed to build on previous modelling work and keep parameters as physiologically realistic as possible to replicate the spontaneous firing activity in the motor cortex. To our knowledge, this is the first physiologically based spiking neural-network model to explore the effects of 3D spatially realistic connectivity on spontaneous neuron firing activity in the motor cortex. The pattern of connectivity is shown to play an important role in the generation of irregular firing dynamics and long-tailed firing distributions of cortical neurons, which could have an impact on criticality and information transmission. With the implementation of local connectivity in a structured cortical circuit, this model links neuroscientific theories of structure to functional network dynamics.

CODE AVAILABILITY & LICENSE

Code and data available at `https://github.com/MunozatABI/MotorCortex`. This work is licensed under a Creative Commons Attribution-NonCommercial 4.0 International License.

ACKNOWLEDGEMENTS

The authors thank Gonzalo Maso Talou and Gurleen Singh for their valuable discussions and Mark Sagar for initial project funding and administration.

FUNDING

L.H. was supported by funding from Callaghan Innovation. The funders had no role in the study design or decision to publish.

CONFLICT OF INTEREST

The authors declare no conflicts of interests.

REFERENCES

[1] Ringach DL. Spontaneous and driven cortical activity: implications for computation. Current Opinion in Neurobiology 2009 8;19:439–444.

[2] Potjans TC, Diesmann M. The cell-type specific cortical microcircuit: Relating structure and activity in a full-scale spiking network model. Cerebral Cortex 2014 mar;24(3):785–806.

[3] Schieber MH. Dissociating motor cortex from the motor. Journal of Physiology 2011 dec;589(23):5613–5624.

[4] Dabrowska PA, Voges N, von Papen M, Ito J, Dahmen D, Riehle A, et al. On the complexity of resting state spiking activity in monkey motor cortex. Cereb Cortex Commun 2021;2(3).

[5] Velliste M, Kennedy SD, Schwartz AB, Whitford AS, Sohn JW, McMorland AJC. Motor cortical correlates of arm resting in the context of a reaching task and implications for prosthetic control. Journal of Neuroscience 2014;34(17):6011–6022.

[6] Churchland MM, Cunningham JP, Kaufman MT, Foster JD, Nuyujukian P, Ryu SI, et al. Neural population dynamics during reaching. Nature 2012;487(7405):51–56.

[7] Sauerbrei BA, Guo JZ, Cohen JD, Mischiati M, Guo W, Kabra M, et al. Cortical pattern generation during dexterous movement is input-driven. Nature 2020;577(7790):386–391.

[8] Deco G, Ponce-Alvarez A, Mantini D, Romani GL, Hagmann P, Corbetta M. Resting-state functional connectivity emerges from structurally and dynamically shaped slow linear fluctuations. Journal of Neuroscience 2013;33(27):11239–11252.

[9] Destexhe A. Intracellular and computational evidence for a dominant role of internal network activity in cortical computations. Current Opinion in Neurobiology 2011 10;21:717–725.

[10] Chen G, Gong P. Computing by modulating spontaneous cortical activity patterns as a mechanism of active visual processing. Nature Communications 2019 dec;10(1).

[11] Tan AYY. Spatial diversity of spontaneous activity in the cortex. Frontiers in Neural Circuits 2015 sep;9(September).

[12] Baker SN, Kilner JM, Pinches EM, Lemon RN. The role of synchrony and oscillations in the motor output. Exp Brain Res 1999;128:109–117.

[13] Tomov P, Pena RFO, Zaks MA, Roque AC. Sustained oscillations, irregular firing, and chaotic dynamics in hierarchical modular networks with mixtures of electrophysiological cell types. Frontiers in Computational Neuroscience 2014 sep;8(SEP).

[14] Hahn G, Petermann T, Havenith MN, Yu S, Singer W, Plenz D, et al. Neuronal Avalanches in Spontaneous Activity In Vivo. J Neurophysiol 2010;104:3312–3322.

[15] Lacey MG, Gooding-Williams G, Prokic EJ, Yamawaki N, Hall SD, Stanford IM, et al. Spike firing and IPSPs in layer V pyramidal neurons during beta oscillations in rat primary motor cortex (M1) in vitro. PLoS ONE 2014 1;9.

[16] Borges FS, Protachevicz PR, Pena RFO, Lameu EL, Higa GSV, Kihara AH, et al. Self-sustained activity of low firing rate in balanced networks. Physica A: Statistical Mechanics and its Applications 2020;537.

[17] Roxin A, Brune N, Hansel D, Mongillo G, van Vreeswijk C. On the distribution of firing rates in networks of cortical neurons. Journal of Neuroscience 2011 nov;31(45):16217–16226.

[18] Buzsaki G, Draguhn A. Neuronal Oscillations in Cortical Networks. Science 2004;304:1926–1930.

[19] Espenhahn S, van Wijk BCM, Rossiter HE, de Berker AO, Redman ND, Rondina J, et al. Cortical beta oscillations are associated with motor performance following visuomotor learning. NeuroImage 2019 7;195:340–353.

[20] Schmidt R, Ruiz MH, Kilavik BE, Lundqvist M, Starr PA, Aron AR. Beta oscillations in working memory, executive control of movement and thought, and sensorimotor function. Journal of Neuroscience 2019 10;39:8231–8238.

[21] Softky WR, Koch C. The Highly Irregular Firing of Cortical Cells Is Inconsistent with Temporal Integration of Random EPSPs. The Journal of Neuroscience 1993;13:334350.

[22] Renart A, de la Rocha J, Bartho P, Hollender L, Parga N, Reyes A, et al. The Asynchronous State in Cortical Circuits. Science 2010;327:587–592.

[23] Ostojic S. Two types of asynchronous activity in networks of excitatory and inhibitory spiking neurons. Nature Neuroscience 2014;17:594–600.

[24] Khanna P, Carmena JM. Beta band oscillations in motor cortex reflect neural population signals that delay movement onset. Elife 2017;.

[25] Habenschuss S, Jonke Z, Maass W. Stochastic Computations in Cortical Microcircuit Models. PLoS Comput Biol 2013;9(11):1003311.

[26] Hawkins J, Ahmad S, Cui Y. A theory of how columns in the neocortex enable learning the structure of the world. Frontiers in Neural Circuits 2017 oct;11(81):1–18.

[27] Shamir M. Emerging principles of population coding: In search for the neural code. Current Opinion in Neurobiology 2014 4;25:140–148.

[28] Markram H, Muller E, Ramaswamy S, Reimann MW, Abdellah M, Sanchez CA, et al. Reconstruction and Simulation of Neocortical Microcircuitry. Cell 2015 oct;163(2):456–492.

[29] Douglas RJ, Martin KAC. Neuronal circuits of the neocortex. Annual Review of Neuroscience 2004;27:419–415.

[30] da Costa NM, Martin KAC. Whose cortical column would that be? Frontiers in Neuroanatomy 2010;.

[31] Hubel DH, Wiesel ATN. Receptive Fields, Binocular Interaction and Functional Architecture in the Cat Visual Cortex. J Physiol 1962;160:106–54.

[32] Ghosh S, Porter R. Morphology of pyramidal neurones in monkey motor cortex and the synaptic actions of their intracortical axon collaterals. The Journal of Physiology 1988 jun;400(1):593–615.

[33] Huntley GW, Jones EG. Relationship of Intrinsic Connections to Forelimb Movement Representations in Monkey Motor Cortex: A Correlative Anatomic and Physiological Study. Journal of Neurophysiology 1991;66:390–413.

[34] Binzegger T, Douglas RJ, Martin KAC. A quantitative map of the circuit of cat primary visual cortex. Journal of Neuroscience 2004;24(39):8441–8453.

[35] Weiler N, Wood L, Yu J, Solla SA, Shepherd GMG. Top-down laminar organization of the excitatory network in motor cortex. Nature Neuroscience 2008 mar;11(3):360–366.

[36] Hooks BM, Hires SA, Zhang YX, Huber D, Petreanu L, Svoboda K, et al. Laminar analysis of excitatory local circuits in vibrissal motor and sensory cortical areas. PLoS Biology 2011;9(1).

[37] Hooks BM, Mao T, Gutnisky DA, Yamawaki N, Svoboda K, Shepherd GMG. Organization of cortical and thalamic input to pyramidal neurons in mouse motor cortex. Journal of Neuroscience 2013 jan;33(2):748–760.

[38] Voges N, Schüz A, Aertsen A, Rotter S, A modeler's view on the spatial structure of intrinsic horizontal connectivity in the neocortex. Elsevier Ltd; 2010.

[39] Bender KJ, Rangel J, Feldman DE. Development of Columnar Topography in the Excitatory Layer 4 to Layer 2/3 Projection in Rat Barrel Cortex. Journal of Neuroscience 2003;23(25).

[40] Shepherd GMG, Stepanyants A, Bureau I, Chklovskii D, Svoboda K. Geometric and functional organization of cortical circuits. Nature Neuroscience 2005 jun;8(6):782–790.

[41] Gong G, He Y, Concha L, Lebel C, Gross DW, Evans AC, et al. Mapping anatomical connectivity patterns of human cerebral cortex using in vivo diffusion tensor imaging tractography. Cerebral Cortex 2009 mar;19(3):524–536.

[42] Senk J, Kriener B, Djurfeldt M, Voges N, Jiang HJ, Schüttler L, et al. Connectivity Concepts in Neuronal Network Modeling. PLOS Computational Biology 2022 10;.

[43] Esser SK, Hill SL, Tononi G. Modeling the Effects of Transcranial Magnetic Stimulation on Cortical Circuits. Journal of Neurophysiology 2005;94:622–639.

[44] Farokhniaee A, Lowery MM. Cortical network effects of subthalamic deep brain stimulation in a thalamo-cortical microcircuit model. Journal of Neural Engineering 2021 oct;18(5).

[45] Moody SL, Zipser D. A model of reaching dynamics in primary motor cortex. Journal of Cognitive Neuroscience 1998;10:35–45.

[46] Manola L, Holsheimer J, Veltink P, Buitenweg JR. Anodal vs cathodal stimulation of motor cortex: A modeling study. Clinical Neurophysiology 2007 feb;118(2):464–474.

[47] Stimberg M, Brette R, Goodman DFM. Brian 2, an intuitive and efficient neural simulator. eLIFE 2019;8:1–41.

[48] Shimoura RO, Kamiji NL, de Oliveira Pena RF, Cordeiro VL, Ceballos CC, Romaro C, et al. Reimplementation of the Potjans-Diesmann cortical microcircuit model: From NEST to Brian. bioRxiv 2018;.

[49] Muralidhar S, Wang Y, Markram H. Synaptic and cellular organization of layer 1 of the developing rat somatosensory cortex. Frontiers in Neuroanatomy 2014;7.

[50] Isaacson JS, Scanziani M. How inhibition shapes cortical activity. Neuron 2011 10;72:231–243.

[51] Holmgren C, Harkany T, Svennenfors B, Zilberter Y. Pyramidal cell communication within local networks in layer 2/3 of rat neocortex. Journal of Physiology 2003 8;551:139–153.

[52] Yoshimura Y, Callaway EM. Fine-scale specificity of cortical networks depends on inhibitory cell type and connectivity. Nature Neuroscience 2005 11;8:1552–1559.

[53] Packer AM, Yuste R. Dense, unspecific connectivity of neocortical parvalbumin-positive interneurons: A canonical microcircuit for inhibition? Journal of Neuroscience 2011 9;31:13260–13271.

[54] Fino E, Packer AM, Yuste R. The logic of inhibitory connectivity in the neocortex. Neuroscientist 2013 6;19:228–237.

[55] Thomson AM, West DC, Wang Y, Bannister AP. Synaptic Connections and Small Circuits Involving Excitatory and Inhibitory Neurons in Layers 2–5 of Adult Rat and Cat Neocortex: Triple Intracellular Recordings and Biocytin Labelling In Vitro. Cerebral Cortex 2002;1047:936–953.

[56] Call CL, Bergles DE. Cortical neurons exhibit diverse myelination patterns that scale between mouse brain regions and regenerate after demyelination. Nature Communications 2021 12;12.

[57] Young NA, Collins CE, Kaas JH. Cell and neuron densities in the primary motor cortex of primates. Frontiers in Neural Circuits 2013 feb;7(30):1–11.

[58] Yamawaki N, Borges K, Suter BA, Harris KD, Shepherd GMG. A genuine layer 4 in motor cortex with prototypical synaptic circuit connectivity. eLife 2014;3:e05422.

[59] Barbas H, Garcia-Cabezas MA. Motor cortex layer 4: less is more. Trends in Neurosciences 2015;38(5):259–261.

[60] Amunts K, Istomin V, Schleicher A, Zilles K. Postnatal development of the human primary motor cortex: a quantitative cytoarchitectonic analysis. Anat Embryol 1995;192:557–571.

[61] Hendry SHC, Schwark HD, Jones EG, Yan J. Numbers and Proportions of GABA-Immunoreactive Neurons in Different Areas of Monkey Cerebral Cortex. The Journal of Neuroscience 1987;7:1503–519.

[62] Bakken TE, Jorstad NL, Hu Q, Lake BB, Tian W, Kalmbach BE, et al. Comparative cellular analysis of motor cortex in human, marmoset and mouse. Nature 2021 oct;598(7879):111–119.

[63] Peters A, Payne BR. Numerical Relationships between Geniculocortical Afferents and Pyramidal Cell Modules in Cat Primary Visual Cortex. Cerebral Cortex 1993;3:69–78.

[64] Braitenberg V, Schuz A. Peters' Rule and White's Exceptions. Berlin, Heidelberg: Springer Berlin Heidelberg; 1998.

[65] Rees CL, Moradi K, Ascoli GA. Weighing the Evidence in Peters' Rule: Does Neuronal Morphology Predict Connectivity? Trends in Neurosciences 2017 2;40:63–71.

[66] Lumer ED, Edelman GM, Tononi G. Neural Dynamics in a Model of the Thalamocortical System. Cerebral Cortex 1997;7:207–227.

[67] Hill S, Tononi G. Modeling Sleep and Wakefulness in the Thalamocortical System. Journal of Neurophysiology 2004 nov;93(3):1671–1698.

[68] Boucsein C, Nawrot MP, Schnepel P, Aertsen A. Beyond the cortical column: Abundance and physiology of horizontal connections imply a strong role for inputs from the surround. Frontiers in Neuroscience 2011;.

[69] van Pelt J, van Ooyen A. Estimating neuronal connectivity from axonal and dendritic density fields. Frontiers in Computational Neuroscience 2013 nov;(NOV).

[70] Collins CE, Turner EC, Sawyer EK, Reed JL, Young NA, Flaherty DK, et al. Cortical cell and neuron density estimates in one chimpanzee hemisphere. Proceedings of the National Academy of Sciences of the United States of America 2016 jan;113(3):740–745.

[71] Crochet S, Petersen CCH. Cortical Dynamics by Layers. Neuron 2009 11;64:298–300.

[72] Beloozerova IN, Sirota MG, Swadlow HA. Activity of Different Classes of Neurons of the Motor Cortex during Locomotion. Journal of Neuroscience 2003;23:1087–1097.

[73] Schiemann J, Puggioni P, Dacre J, Pelko M, Domanski A, VanRossum MCW, et al. Cellular Mechanisms Underlying Behavioral State-Dependent Bidirectional Modulation of Motor Cortex Output. Cell Reports 2015 may;11(8):1319–1330.

[74] Ninomiya T, ichi Inoue K, Hoshi E, Takada M. Layer specificity of inputs from supplementary motor area and dorsal premotor cortex to primary motor cortex in macaque monkeys. Scientific Reports 2019 12;9.

[75] Noda H, Adey WR. Firing Variability in Cat Association Cortex During Sleep and Wakefulness. Brain Research 1970;18:513–526.

[76] Holt GR, Softky WR, Koch C, Douglas RJ. Comparison of Discharge Variability In Vitro and In Vivo in Cat Visual Cortex Neurons. Journal of Neurophysiology 1996;75:1806–14.

[77] Arviv O, Goldstein A, Shriki O. Neuronal avalanches and time-frequency representations in stimulus-evoked activity. Scientific Reports 2019;9(1).

[78] Armstrong DM, Drewt T. Discharges of Pyramidal Tract and Other Motor Cortical Neurones During Locomotion in the Cat. J Physiol 1984;346:471–495.

[79] Estebanez L, Hoffmann D, Voigt BC, Poulet JFA. Parvalbumin-Expressing GABAergic Neurons in Primary Motor Cortex Signal Reaching. Cell Reports 2017;20(2):308–318.

[80] Jensen O, Goel P, Kopell N, Pohja M, Hari R, Ermentrout B. On the human sensorimotor-cortex beta rhythm: Sources and modeling. NeuroImage 2005 jun;26(2):347–355.

[81] Kilavik BE, Zaepffel M, Brovelli A, MacKay WA, Riehle A. The ups and downs of beta oscillations in sensorimotor cortex. Experimental Neurology 2013 7;245:15–26.

[82] Barone J, Rossiter HE. Understanding the Role of Sensorimotor Beta Oscillations. Frontiers in Systems Neuroscience 2021;15.

[83] Shadlen MN, Newsome WT. Noise, neural codes and cortical organization. Current Opinion in Neurobiology 1994;4:569–579.

[84] Chen Y, Zhang H, Wang H, Yu L, Chen Y. The Role of Coincidence-Detector Neurons in the Reliability and Precision of Subthreshold Signal Detection in Noise. PLoS ONE 2013 2;8.

[85] deCharms RC. Information coding in the cortex by independent or coordinated populations. Proc Natl Acad Sci 1998;95:15166–15168.

[86] Beggs JM, Timme N. Being critical of criticality in the brain. Frontiers in Physiology 2012;3.

[87] Chialvo DR. Emergent complex neural dynamics. Nature Physics 2010;6:744–750.

[88] Deco G, Jirsa VK. Ongoing cortical activity at rest: Criticality, multistability, and ghost attractors. Journal of Neuroscience 2012 3;32:3366–3375.

[89] Shew WL, Plenz D. The functional benefits of criticality in the cortex. Neuroscientist 2013 2;19:88–100.

[90] Zhou S, Yu Y. Synaptic E-I balance underlies efficient neural coding. Frontiers in Neuroscience 2018 2;12.

[91] Deco G, Ponce-Alvarez A, Hagmann P, Romani GL, Mantini D, Corbetta M. How local excitation-inhibition ratio impacts the whole brain dynamics. Journal of Neuroscience 2014;34:7886–7898.

[92] Kumar A, Rotter S, Aertsen A. Conditions for propagating synchronous spiking and asynchronous firing rates in a cortical network model. Journal of Neuroscience 2008 may;28(20):5268–5280.

[93] van Vreeswijk C, Sompolinsky H. Chaos in Neuronal Networks with Balanced Excitatory and Inhibitory Activity. Science 1996;274:1724–1726.

[94] Brunel N. Dynamics of Sparsely Connected Networks of Excitatory and Inhibitory Spiking Neurons. Journal of Computational Neuroscience 2000;8:183–208.

[95] Westlake KP, Nagarajan SS. Functional connectivity in relation to motor performance and recovery after stroke. Frontiers in Systems Neuroscience 2011;5:8.

[96] Mehring C, Hehl U, Kubo M, Diesmann M, Aertsen A. Activity dynamics and propagation of synchronous spiking in locally connected random networks. Biological Cybernetics 2003 may;88(5):395–408.

[97] Yger P, El Boustani S, Destexhe A, Frégnac Y. Topologically invariant macroscopic statistics in balanced networks of conductance-based integrate-and-fire neurons. Journal of Computational Neuroscience 2011;31(2):229–245.

[98] Voges N, Perrinet L. Complex dynamics in recurrent cortical networks based on spatially realistic connectivities. Frontiers in Computational Neuroscience 2012 jul;6(JUL).

[99] Callaway EM. Cell type specificity of local cortical connections. Journal of Neurocytology 2002;31:231–237.

[100] Udvary D, Harth P, Macke JH, Hege HC, de Kock CPJ, Sakmann B, et al. The impact of neuron morphology on cortical network architecture. Cell Reports 2022 apr;39(2).

[101] White EL. Specificity of cortical synaptic connectivity: Emphasis on perspectives gained from quantitative electron microscopy. Journal of Neurocytology 2002;31:195–202.

[102] Mountcastle VB. Modality and Topographic Properties of Single Neurons of Cat's Somatic Sensory Cortex. Journal of Physiology 1957;20(4):408–434.

[103] Horton JG, Adams DL. The cortical column: A structure without a function. Philosophical Transactions of the Royal Society B: Biological Sciences 2005 4;360:837–862.

[104] Haueis P. The life of the cortical column: opening the domain of functional architecture of the cortex (1955–1981). History and Philosophy of the Life Sciences 2016 sep;38(3).

[105] Schwalger T, Deger M, Gerstner W. Towards a theory of cortical columns: From spiking neurons to interacting neural populations of finite size. PLoS Computational Biology 2017 apr;13(4).

[106] Georgopoulos AP, Schwartz AB, Kettner RE. Neuronal Population Coding of Movement Direction. Science 1986;233:1416–1419.

[107] Amirikian B, Georgopoulos AP. Modular organization of directionally tuned cells in the motor cortex: Is there a short-range order? Proc Natl Acad Sci USA 2003;100:12474–12479. www.pnas.orgcgidoi10.1073pnas.2037719100.

[108] Georgopoulos AP, Stefanis CN. Local shaping of function in the motor cortex: Motor contrast, directional tuning. Brain Research Reviews 2007;55:383–389.

[109] Hatsopoulos NG. Columnar organization in the motor cortex. Cortex 2010;46:270–271.

[110] Zeldenrust F, Wadman WJ, Englitz B. Neural coding with bursts—Current state and future perspectives. Frontiers in Computational Neuroscience 2018 7;12.

[111] Masquelier T, Deco G. Network Bursting Dynamics in Excitatory Cortical Neuron Cultures Results from the Combination of Different Adaptive Mechanism. PLoS ONE 2013 10;8.

[112] Zhao Z, Li L, Gu H. Different dynamical behaviors induced by slow excitatory feedback for type II and III excitabilities. Scientific Reports 2020 12;10.

[113] Markram H, Toledo-Rodriguez M, Wang Y, Gupta A, Silberberg G, Wu C. Interneurons of the neocortical inhibitory system. Nature Reviews Neuroscience 2004 10;5:793–807.

[114] Sussillo D, Churchland M, Kaufman M, Shenoy K. A Neural Network that Finds a Naturalistic Solution for the Production of Muscle Activity. Nature Neuroscience 2016;18:1025 – 1033.

[115] Michaels JA, Schaffelhofer S, Agudelo-Toro A, Scherberger H. A neural network model of flexible grasp movement generation. bioRxiv 2019;.

[116] Spüler M, Nagel S, Rosenstiel W. A spiking neuronal model learning a motor control task by reinforcement learning and structural synaptic plasticity. In: Proceedings of the International Joint Conference on Neural Networks, vol. 2015-September Institute of Electrical and Electronics Engineers Inc.; 2015. .

[117] Romeny BMTH, Gon JJDVD, Gielen CCAM. Relation between Location of a Motor Unit in the Human Biceps Brachii and Its Critical Firing Levels for Different Tasks. Experimental Neurology 1984;85.

[118] Marshall NJ, Glaser JI, Trautmann EM, Amematsro EA, Perkins SM, Shadlen MN, et al. Flexible neural control of motor units. Nature Neuroscience 2022 11;25:1492–1504. https://www.nature.com/articles/s41593-022-01165-8.

[119] Logiaco L, Abbott LF, Escola S. Thalamic control of cortical dynamics in a model of flexible motor sequencing. Cell Reports 2021 6;35.

[120] Shenoy KV, Sahani M, Churchland MM. Cortical Control of Arm Movements: A Dynamical Systems Perspective. Annual Review of Neuroscience 2013 7;36:337–359.